MAGNETIC LATITUDE EFFECTS IN THE SOLAR WIND

C. Richard Winge, Jr., and Paul J. Coleman, Jr.

ABSTRACT

The Weber-Davis model of the solar wind is generalized to include the effects of latitude. The principal assumptions of high electrical conductivity, rotational symmetry, the polytropic relation between pressure and density, and a flow-alined field in a system rotating with the sun, are retained. An approximate solution to the resulting equations for spherical boundary conditions at the base of the corona indicates a small component of latitudinal flow toward the solar poles at large distances from the sun as a result of latitudinal magnetic forces.

The purpose of this paper is to demonstrate that even with spherically symmetric boundary conditions at the base of the corona, the magnetic field introduces a small latitude effect in the solar wind that should be measurably significant at large distances. As motivation for a more general development it is useful to consider the magnetic forces predicted by the spiral field approximation of *Parker* [1958]. The magnetic force per unit mass for this model is

$$(\nabla \times \mathbf{B}) \times \mathbf{B}/(4\pi\rho) = -\nabla[(B_O^2/4\pi\rho_O)\sin^2\theta] \qquad (1)$$

where B_O and ρ_O are reference values for the magnetic field and density. The total force per unit mass is then given by the negative gradient of the sum of the thermal energy per unit mass, the gravitational energy per unit mass, and the magnetic energy per unit mass (eq. (1)). The thermal term is assumed to be falling adiabatically toward zero at large distances, and the gravitational term is decreasing toward zero; however, for spherical boundary conditions on B_O and ρ_O, the magnetic term depends upon $\sin^2\theta$ and does not decrease explicitly with r. This suggests that changes in momentum at large distances may be dominated by the magnetic field.

The authors are with the Department of Planetary and Space Science and Institute of Geophysics and Planetary Physics, University of California, Los Angeles, California.

The magnetic torque per unit mass for this model is then

$$\boldsymbol{\tau} = \mathbf{r} \times (d\mathbf{V}/dt) = -(B_O^2/4\pi\rho_O)\sin\theta\cos\theta\,\hat{\phi} \qquad (2)$$

which acts to drive the plasma toward the poles, producing a nonzero component of the θ component of velocity V_θ. For infinite electrical conductivity, the presence of a finite component of V_θ implies a finite component of B_θ through the process of convection. The assumed field is therefore inconsistent with respect to latitude and requires a more general treatment. It should be noted that the magnetic stress given by this model results because of the ϕ component of the magnetic field. Since this winding of the field is due to solar rotation, the effect demonstrated here may be expected to persist in a more general treatment.

The approach to be described here is identical with that of *Weber and Davis* [1967] except that the equations are generalized to include the effects of latitude through the development of the normal component of momentum. We begin with the steady-state flow equations subject to the following assumptions: (1) neglect viscosity, (2) isotropic thermal conductivity, (3) infinite electrical conductivity, (4) equal electron and proton temperatures, and (5) energy equation may be replaced by the polytropic law. We further assume rotational symmetry and that

the magnetic field and flow velocity are parallel in a reference system rotating with the sun. A flow-alined field may be generally represented by

$$\mathbf{B} = \kappa \rho \mathbf{U} \tag{3}$$

where $\mathbf{U} = \mathbf{V} - \omega_S r \sin\theta \, \hat{\phi}$ is the flow velocity in the rotating system, $\mathbf{V}$ is the flow velocity in a fixed system of reference, ρ is the mass density, and ω_S is the solar rotation rate. The condition $\nabla \cdot \mathbf{B} = 0$, combined with the equation of continuity, requires κ to be a streamline constant. The physical meaning of κ is obtained by noting that the quantity $\kappa^2 \rho / 4\pi$ must be unity at the Alfvén point, or $\kappa^2 = 4\pi/\rho_A$ where ρ_A is the density at the Alfvén point.

With rotational symmetry the ϕ component of the momentum equation may be directly integrated to obtain V_ϕ as a function of r, θ, and ρ, which when combined with the magnetic field as a function of velocity and density (eq. (3)), reduces the problem to one of two-dimensional flow in the $r\theta$ plane. Given boundary conditions, the unknowns at a general point r, θ are ρ, V_r, and V_θ, which are determined by the equation of continuity, the parallel component of momentum (Bernoulli's equation), and the normal component of momentum. The problem is complicated by the presence of three critical surfaces corresponding to the fast, slow, and Alfvén modes of propagation in the medium.

A particular streamline will be designated by specifying its coordinate θ_o at the base of the corona, which is constant along the streamline. There are six required boundary values that must be specified or determined as functions of θ_o at the coronal base: $T_o(\theta_o)$, $\rho_o(\theta_o)$, $V_{ro}(\theta_o)$, $V_{\theta o}(\theta_o)$, $\kappa(\theta_o)$, and the total ϕ component of angular momentum along the streamline $L(\theta_o)$. The requirement that the velocity components be finite at the three critical surfaces supplies three of the required boundary conditions for $V_{\theta o}$, κ, and L. Further, if $B_o(\theta_o)$ is specified, then V_{ro} may be determined through equation (3). Hence, we chose to specify $T_o(\theta_o)$, $\rho_o(\theta_o)$, and $B_o(\theta_o)$, the magnitude of the total magnetic field at the coronal base.

We find that the best way to cope with the critical surfaces is to integrate the equations along a streamline until the critical point is encountered and then to vary a boundary condition until the streamline that passes through is determined. Because of the differential form of the equations, integration along a streamline is possible only if the previous neighboring streamline is known. Hence, to start the integration, the polar limit of the equations is required. However, the equations at the pole are not closed and an assumption is necessary to obtain the polar limit. A complete solution to the problem is possible through a process of iteration over the entire set of streamlines; however, techniques we have been able to devise thus far are too costly.

As a first approximation to the solution, we chose to close the equations with the assumption

$$V_\theta / V_r = -\left\{ r [df(r)/dr] / f(r) \right\} \sin\theta \cos\theta \tag{4}$$

which integrates to

$$\tan\theta_o = f(r) \tan\theta \tag{5}$$

Equation (4) is the lowest order θ dependence for which V_θ is zero at both the equator and the pole. The radial function f(r) specifies the shape of the streamlines. Radial flow in the $r\theta$ plane is given by f(r) = 1 and df(r)/dr = 0. The function f(r) is determined by integration of the limit of the normal component of momentum along the polar stream line. In the polar limit we have

$$\partial V_\theta / \partial\theta = -V_r [r \, df(r)/dr] / f(r) \qquad (\theta = 0) \tag{6}$$

$$\partial\theta_o / \partial\theta = f(r) \tag{7}$$

The results of equations (4) and (5) and the polar integration of $f(r)$ for two sets of constant temperature, density, and magnetic field at the coronal base are presented in tables 1 through 4 and figure 1. Figure 1 shows the radial dependence of V_θ along a streamline for the two sets of boundary conditions; tables 1 and 2 tabulate the resulting values at 1 AU, and tables 3 and 4 tabulate the corresponding critical surfaces.

The function $f(r)$ obtained at the pole is not overly sensitive to reasonable changes in the assumed model to close the equations for constant boundary conditions. The general shape of the curve results from the physics of the problem and is maintained. Since V_θ for $\theta_o = 10°$ may be obtained directly from the polar solution through equation (6), this curve should be in close agreement with an exact solution. The curves for $\theta_o > 10°$, however, are contingent upon how well the assumption contained in equation (4) approximates the normal component of momentum at lower latitudes.

The results presented here indicate a modest latitudinal flow toward the poles due to magnetic stresses, which persist out to very large distances from the sun for spherical boundary conditions at the corona. Associated with this flow is a θ component of the magnetic field. The radial flow parameters are not

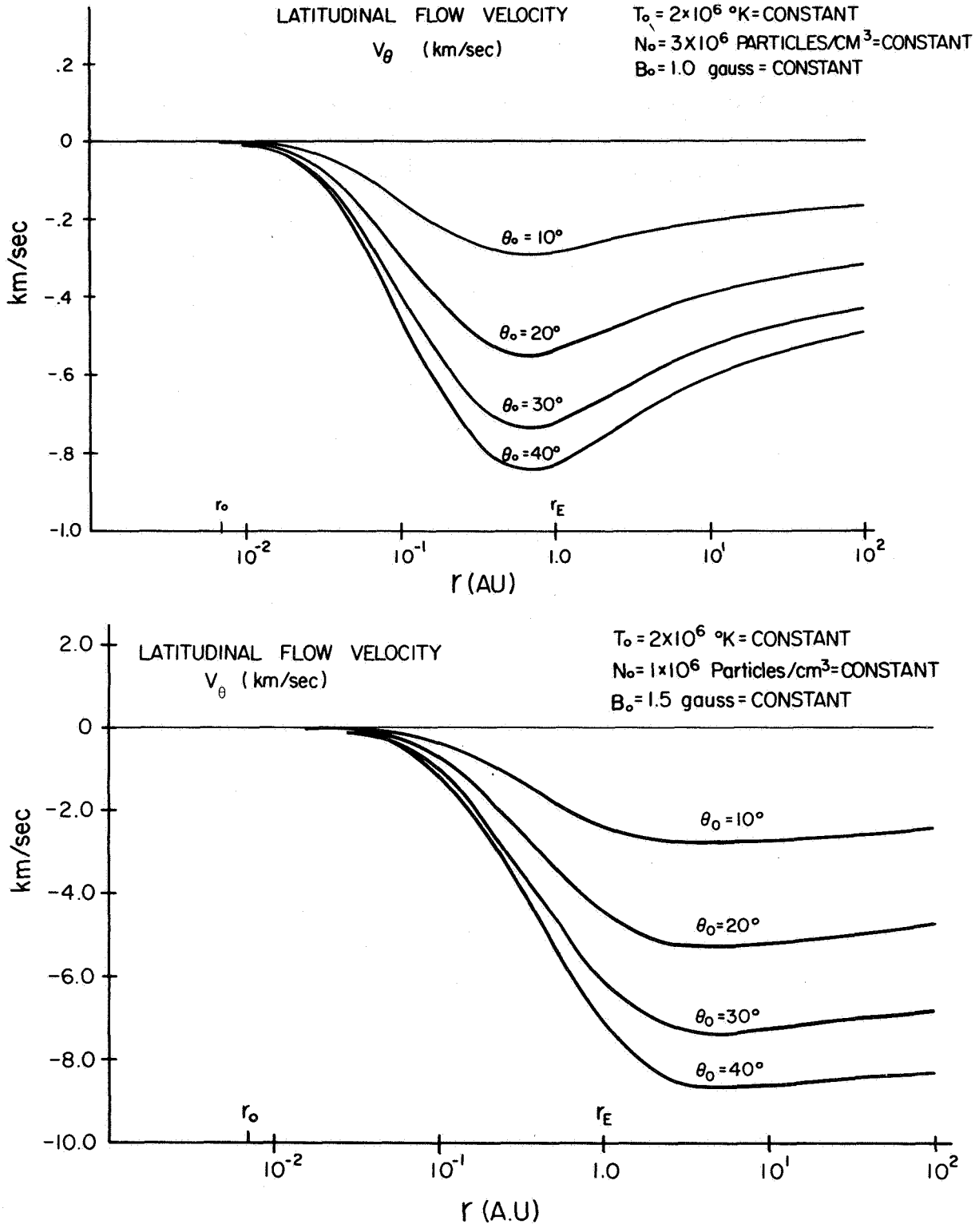

Figure 1. *Latitudinal flow velocity for two sets of constant boundary conditions at the coronal base, $r_O = 1.0\times10^{11}$ cm. Curves for $\theta_O = 50°$, 60°, 70° and 80° are nearly identical with the displayed curves for 40°, 30°, 20° and 10°, respectively, and are not shown.*

Table 1. *Predicted values at 1 AU*

[Constant coronal boundary conditions: $T_O = 2\times10^6$ °K, $N_O = 3\times10^6$ particles/cm^3, $B_O = 1$ gauss]

θ_O, deg	θ, deg	Velocity, km/sec			Magnetic field, 10^{-5} gauss			Density, protons/cm^3	Temperature, °K
		V_r	V_θ	V_ϕ	B_r	B_θ/B_r	B_ϕ/B_r		
10	9.88	403	-0.28	0.19	3.57	-7.06×10^{-4}	-0.19	13.6	3.16×10^5
20	19.78	403	-0.54	0.37	3.57	-1.33×10^{-3}	-0.38	13.6	3.16×10^5
30	29.70	403	-0.72	0.53	3.56	-1.80×10^{-3}	-0.55	13.6	3.16×10^5
40	39.65	403	-0.83	0.68	3.55	-2.05×10^{-3}	-0.71	13.5	3.16×10^5
50	49.65	403	-0.83	0.81	3.54	-2.06×10^{-3}	-0.85	13.5	3.16×10^5
60	59.69	403	-0.73	0.91	3.53	-1.82×10^{-3}	-0.96	13.5	3.15×10^5
70	69.77	404	-0.55	0.98	3.52	-1.35×10^{-3}	-1.04	13.5	3.15×10^5
80	79.88	404	-0.29	1.03	3.51	-7.22×10^{-4}	-1.09	13.5	3.15×10^5

Table 2. *Predicted values at 1 AU*

[Constant coronal boundary conditions: $T_O = 2\times10^6$ °K, $N_O = 1\times10^6$ particles/cm^3, $B_O = 1.5$ gauss]

θ_O, deg	θ, deg	Velocity, km/sec			Magnetic field, 10^{-5} gauss			Density, protons/cm^3	Temperature, °K
		V_r	V_θ	V_ϕ	B_r	B_θ/B_r	B_ϕ/B_r		
10	9.48	402	-2.37	0.60	6.75	-5.89×10^{-3}	-0.18	5.85	3.28×10^5
20	19.01	402	-4.50	1.16	6.70	-1.12×10^{-2}	-0.36	5.83	3.28×10^5
30	28.66	403	-6.15	1.64	6.64	-1.53×10^{-2}	-0.53	5.80	3.28×10^5
40	38.46	403	-7.13	2.05	6.56	-1.77×10^{-2}	-0.69	5.75	3.27×10^5
50	48.44	403	-7.27	2.34	6.47	-1.80×10^{-2}	-0.83	5.71	3.27×10^5
60	58.62	404	-6.51	2.56	6.39	-1.61×10^{-2}	-0.94	5.66	3.27×10^5
70	68.98	404	-4.81	2.69	6.32	-1.19×10^{-2}	-1.03	5.62	3.26×10^5
80	79.45	404	-2.64	2.78	6.27	-6.54×10^{-3}	-1.09	5.59	3.26×10^5

Table 3. *Critical surfaces*

[Constant coronal boundary conditions: $T_O = 2\times10^6$ °K, $N_O = 3\times10^6$ particles/cm^3, $B_O = 1$ gauss]

θ_O, deg	Slow mode		Alfvén mode		Fast mode	
	r_S, solar radii	θ_S, deg	r_A, solar radii	θ_A, deg	r_f, solar radii	θ_f, deg
10	4.012	9.997	15.233	9.979	15.239	9.979
20	4.011	19.994	15.226	19.961	15.236	19.961
30	4.010	29.992	15.211	29.947	15.233	29.947
40	4.008	39.991	15.194	39.940	15.230	39.940
50	4.006	49.991	15.174	49.940	15.226	49.940
60	4.004	59.992	15.159	59.947	15.224	59.947
70	4.003	69.994	15.144	69.961	15.221	69.961
80	4.002	79.997	15.136	79.979	15.220	79.979

Table 4. *Critical surfaces*

[Constant coronal boundary conditions: $T_O = 2\times10^6$ °K, $N_O = 1\times10^6$ particles/cm^3, $B_O = 1.5$ gauss]

θ_O, deg	Slow mode		Alfvén mode		Fast mode	
	r_S, solar radii	θ_S, deg	r_A, solar radii	θ_A, deg	r_f, solar radii	θ_f, deg
10	4.015	9.997	36.043	9.895	36.067	9.895
20	4.013	19.994	35.931	19.803	36.027	19.803
30	4.011	29.992	35.773	29.736	35.977	29.734
40	4.008	39.991	35.578	39.701	35.914	39.698
50	4.003	49.991	35.354	49.703	35.827	49.698
60	4.001	59.992	35.178	59.740	35.781	59.734
70	3.999	69.994	35.020	69.805	35.731	69.803
80	3.997	79.997	34.931	79.896	35.703	79.895

significantly different from the Parker or Weber-Davis models for latitudinal flow velocities up to about 10 km/sec.

ACKNOWLEDGMENTS

This work was supported in part by the National Aeronautics and Space Administration under research grant NGR 05-007-065. A portion of the computer costs was covered by the Regents of the University of California. The authors are grateful to G. L. Siscoe and G. Schubert for helpful discussions.

REFERENCES

Parker, E. N.: Dynamics of the Interplanetary Gas and Magnetic Field. *Astrophys. J.*, Vol. 128, 1958, p. 664.

Weber, E.; and Davis, L., Jr.: The Angular Momentum of the Solar Wind. *Astrophys. J.*, Vol. 148, 1967, p. 217.